Emergent symmetry breaking during the foraging collective activity by ants

A. L. Ballinas-Hernández

Complejo Regional Centro sede San José Chiapa, Benemérita Universidad Autónoma de Puebla, Calle 2 sur S/N, Ciudad Modelo, San José Chiapa, C.P. 75010 Puebla, México.
e-mail: analuisa.ballinas@correo.buap.mx

M. Rangel-Galván and N. Villa-Ruano

Dirección de Innovación y Transferencia de Conocimiento, Benemérita Universidad Autónoma de Puebla ICUAP, 24 Sur y San Claudio, Ciudad Universitaria, Puebla, C.P. 72570 Puebla, México.
e-mail: maricruz.rangelgalvan@viep.com, necho82@yahoo.com.mx

V. Rangel-Galván

Complejo Regional Centro sede Acatzingo, Benemérita Universidad Autónoma de Puebla, Carretera Federal Nopalucan Km 3.36, Col. Apipilolco, Acatzingo, C.P. 75150 Puebla, México.
e-mail: violeta.rangel@alumno.buap.mx

Received 5 May 2025; accepted 4 August 2025

This study analyzes a system of nonlinear differential equations associated with the number of foraging ants visiting two identical exploitation sources in a static environment. Steady-state solutions correspond to establishing pheromone trails sustained after the colony density reaches a critical size. In the quasi-steady-state approximation, the model reduces to a single-variable symmetry description. After including additive white noise perturbations, the scheme becomes a Langevin equation. Solutions to this equation suggest that the processes underlying the collective task are associated with an order (recruitment-abandonment) - disorder (successful exploration) parameter that varies as a rational homographic function concerning the control parameter of the model. We find that intrinsic random disturbances, produced by successful foragers, break the symmetry of an equal number of ants in each option, leading to preferential visits to one of the two food sources. We also observe that the behavior of the order-disorder parameter is strongly dependent on changes in the colony size. In general, the stability of consensus in collective decision-making increases with increasing noise intensity.

Keywords: Ants' foraging; symmetry breaking; Langevin equation; collective decision-making.

DOI: https://doi.org/10.31349/RevMexFis.72.011701

1. Introduction

Insect societies organize their survival activities in a decentralized manner. The main well-identified collective tasks are nest building and foraging for materials and food. The latter event occurs when part of the population of an ant colony leaves the nest to explore the surrounding environment in search of food. The first foraging stage is completed when some successful explorers, who find food through independent foraging, return to deposit their food and recruit other nestmates to perform the collective task. Many foraging ant colonies use pheromone trails to guide their nestmates to food sources. In the second stage, the ants reinforce the pheromone trail by leaving their signals during repeated return trips to the nest. This is necessary to ensure that the trails do not disappear. In the third task stage, the recruitment process becomes saturated, probably due to overcrowding of food sources or sensory saturation of the individuals. Suddenly, the recruited ants lose their pheromone trail more easily [1, 2].

Once the pheromone trails are established from the nest to food sources, some scout ants are attracted to the foraging task. This recruitment process is reinforced by a positive feedback mechanism [2]. Furthermore, a negative feedback mechanism develops during the process of abandoning the task, which is mandatory to restrict recruitment and prevent it from increasing indefinitely [3]. After the foraging task is established, a recruitment-abandonment balance occurs, a steady-state is reached, and the average number of foragers remains unchanged on the trails as long as food sources are not depleted.

Quantitative studies of collective foraging require experimental setups capable of uncovering the underlying mechanisms of behavior under controlled conditions. In fact, some authors found that the foraging population is a nonlinear function of colony size and that a minimum number of ants is required to maintain a pheromone trail [1]. Furthermore, experiments show that ant colonies that exclusively use pheromone trails are unable to maintain and sustain these trails in an organized manner, even if the food sources are in an area close to the nest.

A foraging ant colony could regularly exploit one or more food sources. In this case, indirect communication via pheromone trails efficiently allocates a specific number of foragers to each option. The decentralized process of organizing the task and assigning several foragers involves collec-

tive decision-making by the colony. Various studies have observed that the pheromone trails are more strongly biased toward the most profitable food sources when the colony plans to visit several options simultaneously [2, 4, 5].

Currently, it is not yet established whether pheromone-guided foraging allows the colony to adapt to sudden changes in dynamic environments with ephemeral food sources. Once again, collective decision-making mechanisms that allow the colony to allocate several foragers to each option remain elusive to explain [4, 6]. In this sense, experiments by Ref. [1] confirm that a Pheidole megacephala colony can make appropriate collective decisions toward selecting the most profitable options. Some colonies of ants, with many individuals, implement pheromone recruitment and direct mass recruitment mechanisms; for example, colonies of Tetramorium caespitum and Camponotus socius incorporate both mechanisms. This dual mechanism allows the colony to establish pheromone trails quickly.

Authors in Ref. [2] found that the recruitment by pheromone trails is a highly nonlinear phenomenon, due to proportional changes in the amount of pheromone deposited that induce excessive responses in the allocation of foragers among different options. This has been experimentally confirmed in colonies of the pharaoh's ant, Monomorium pharaonis, when they visit two food sources with the same or different profitability [2]. Experiments show that the colony can efficiently allocate adequate foragers among different food sources using only indirect communication via pheromone trails [3]. On average, the allocation of foragers is the same regardless of whether the colony visits one or two options with the same or different profitability. The initial conditions of forager allocation determine whether they visit equally or prefer to exploit one of the options, specifically [2].

Some researchers established that when an ant colony simultaneously exploits several food sources, decentralized self-organization mechanisms are incorporated, and collective decision-making is based only on local information of individuals [5, 7, 8]. Experimental results on the foraging of a Pheidole megacephala colony show that deterministic steady-state processes and random noise perturbations on the system work together during the collective task to give the colony adaptability to the environment. Furthermore, it is known that a certain level of noise is a necessary element in collective self-organization decision-making for the allocation of forage among different options [4, 9, 10]. In fact, the authors assume that allocation emerges from competition between two recruitment processes, one based on persistent pheromone trails and another based on random recruitment stimuli emitted by successful explorers. It is found that slight modifications at the nest entrance affect collective decision-making on the number of foragers assigned to each food source [6].

In this paper, we consider a macroscopic model of ant colony foraging based on a system of nonlinear recruitment-abandonment balance equations. These dynamic equations are characterized by a set of steady-state solutions associated with the establishment of pheromone trails. The colony allocates some foragers consistent with a competition of coupled positive and negative feedback processes in these steady-states. The system remains steady until internal or external perturbations trigger a transition between different options [2, 3, 9, 10].

To simplify the model, we consider the successful exploration term a noise disturbance intrinsic to the foraging colony. This consideration is compatible with the effects of the variable number of individuals finding food sources through independent random searches. As we mentioned earlier, noise disturbance during foraging is an important functional element for colony adaptation to the simultaneous exploitation of several food sources. In general, the noise effect is associated with a symmetry breaking toward the most profitable food source. Random fluctuations can change foraging behavior by modifying pheromone levels and affecting the degree of preference among several options [4, 9, 10].

Specifically, we propose a representation of the allocation of forager numbers across two equally profitable food sources, based on a description of the macroscopic recruitment-abandonment balance. We find pertinent insights into the mechanisms underlying the phenomenon of symmetry breaking in the number of foragers of each option, due to intrinsic noise caused by successful forager explorers. The results are explained in terms of the statistical analysis of precision and stability in collective decision-making among several options associated with symmetry breaking induced by the intrinsic noise in the system.

2. Basic equations

During the development of pheromone-guided foraging activity by an ant colony, two collective mechanisms are presented that function as regulators of the task: Recruitment (R) occurs when a slight variation in the intensity of the pheromone trail releases a self-catalytic process that leads to an increase in the mass of the foraging population, and abandonment (A) of the task begins when the pheromone concentration saturates s, the sensitivity of individual ants. Another circumstance of abandonment is overcrowding food sources [11]. The fraction of foragers who cannot stay on the trail of the entire path abandons the task to incorporate themselves into the group of scout ants. This last group includes successful explorers (E) who return to the nest with food found by independent random searches.

The proposed model considers that the rate of change in the number of foraging ants (x) obeys a macroscopic balance equation of three tasks that a colony of size (n) performs when visiting food sources [1, 2],

$$\frac{dx}{dt} = (R(x) - A(x)) + E(x). \tag{1}$$

We assumed temporal dependence on the variable $x = x(t)$. In addition, we consider contributions of recruitment $R(x)$, abandonment $A(x)$ of pheromone trail, and successful

FIGURE 1. Collective foraging activity of an ant colony.

exploration $E(x)$ as the main characteristics of the collective foraging task (see Fig. 1).

The systematic component is a balance of recruitment-abandonment processes, in a competition or interplay of positive feedback mechanisms versus negative feedback, which develop during the collective task as long-term dynamics. At the same time, the model assumes that successful explorers maintain, on average, a stable population consisting of unemployed ants, novice explorers with incomplete trips, and foragers that abandon the pheromone trails. This group is the random component, which contributes a dynamic of abrupt, small-amplitude changes in the forager population (task tuning), producing short-term effects.

We observed a large population of scouts during trail formation. Recruitment has limited efficiency due to pheromone evaporation. Furthermore, at a certain level, the intensity of the pheromone trail saturates the sensitivity of individual foraging ants. If s is the saturation coefficient of the ability to perceive recruitment signals, the efficiency of each ant (subscript 1) in following the entire trail is [11],

$$R_1(x) = \frac{x}{s+x}. \tag{2}$$

Figure 2 shows that recruitment per ant $R_1(x)$ is a rational homographic function with a vertical asymptote ($x = -s$), a horizontal asymptote ($y = 1$), passing through the point $(0, 0)$. Three values of the saturation coefficient are considered ($s = 1, 10, 20$).

On the other hand, due to sensitivity saturation, the weakening of the pheromone trail by evaporation, and overcrowding at food sources, part of the foraging ant group fails to follow the entire trail to the food source. This group abandons the collective task of exploring other sources, returns to the nest, or defends the colony from competitors. The abandonment task rate per individual is a complementary process to recruitment $A_1(x) = 1 - R_1(x)$, which is the rate at which an ant loses the trail of following the entire trail and abandons the foraging task. This function is given by Eq. (3),

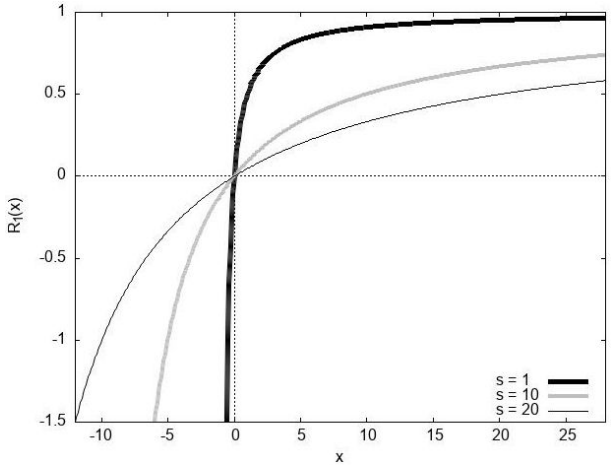

FIGURE 2. Recruitment function per individual.

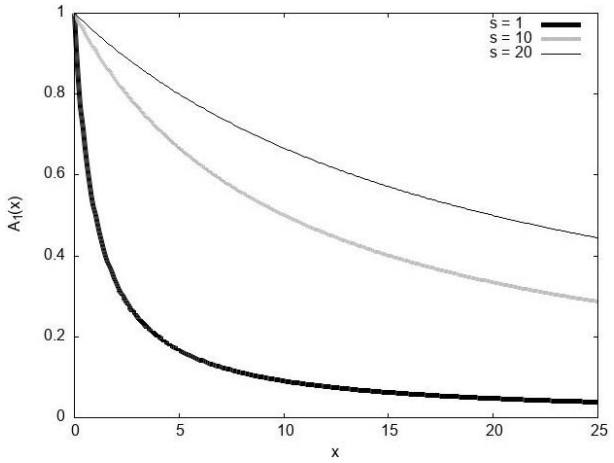

FIGURE 3. The task abandonment function per individual.

$$A_1(x) = \frac{s}{s+x}. \tag{3}$$

Figure 3 shows the abandonment function $A_1(x)$ per ant. This function decreases with the increase in the number of foragers on the pheromone trail, and therefore with the intensity of the pheromone trails. Three values of the saturation coefficient are considered ($s = 1, 10, 20$).

Each term in Eq. (1) corresponds to the macroscopic mass variables $R(x)$, $A(x)$, and $E(x)$. These contributions are constructed under the assumption that population interaction is an autocatalytic process that incorporates individuals into the collective task, which is represented as the product of concentrations.

The recruitment term for the incorporation of unemployed ants into the trails is constructed as the interaction of two populations, the foraging ants (x), and the free scouts susceptible to recruitment ($n - x$). In fact, foragers are recruited into groups at a rate of $R(x) = \beta x(n - x)$, which is proportional to the product of foraging ants and unemployed ants.

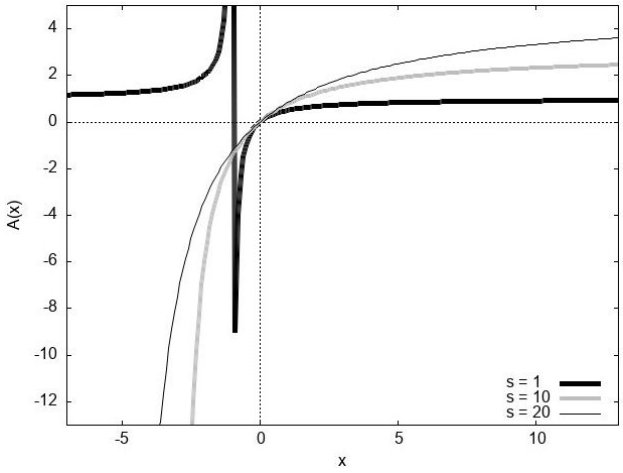

FIGURE 4. Mass task abandonment function.

The population of foragers who abandon the task in mass, once the trail has been formed, according to Eq. (3), is given by Eq. (4),

$$A(x) = A_1(x)x = \frac{s}{s+x}x. \tag{4}$$

Figure 4 shows that the population abandonment rate $A(x)$ is a rational homographic function with a vertical asymptote ($x = -s$) and a horizontal asymptote ($y = s$) passing through the point $(0, 0)$. Three values of the saturation coefficient are considered ($s = 1, 10, 20$). This figure shows that the parameter s is the maximum abandonment rate due to loss of the pheromone trail.

At this point, a fraction of successful explorers $\alpha(n-x)$ reach the food source through random searches independent of the pheromone trail. When considering the above assessments, Eq. (1) becomes the food foraging balance equation, which we refer to as the Beekman equation,

$$\frac{dx}{dt} = \left(\beta(n-x) - \frac{s}{s+x}\right)x + \alpha(n-x). \tag{5}$$

The first term, in parentheses, corresponds to the deterministic part of the foraging task when the pheromone trail is well established, while the second term corresponds to foraging due to independent searches by successful explorers (see Ref. [1]).

3. Quasi-stationary state

If an ant colony visits two food sources A and B simultaneously, Eq. (5) is used to determine a system of nonlinear differential equations associated with the collective task. In fact, if we consider that $x = x_A + x_B$ in this equation, where the number of foragers of A and B is given by x_A and x_B respectively, and subsequently separate the contributions of the corresponding state variables of each option, the following system of nonlinear differential equations is established,

$$\frac{dx_A}{dt} = \left(\beta(n-(x_A+x_B)) - \frac{s}{s+(x_A+x_B)}\right)x_A + \alpha_A(n-(x_A+x_B)), \tag{6}$$

$$\frac{dx_B}{dt} = \left(\beta(n-(x_A+x_B)) - \frac{s}{s+(x_A+x_B)}\right)x_B + \alpha_B(n-(x_A+x_B)). \tag{7}$$

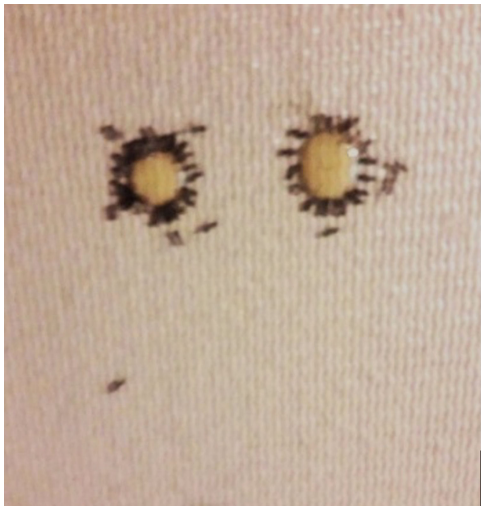

FIGURE 5. The ant colony visits two food sources simultaneously.

This model incorporates blurred pheromone trails as expected to occur in open environments (see Fig. 5). The individual sensitivity saturation is due to the pheromone deposited by the total number of foragers observed in the abandonment term of the task.

In Eqs. (6) and (7), it is assumed that the recruitment-abandonment coefficients β and s do not depend on the selection of A or B during the foraging ant allocation, given that food sources are identical [2]. At first, $\alpha_A = \alpha_B$, however, to preserve exploration contributions in Sec. 4, where the exploration coefficient is a random variable that generates intrinsic system noise, we change this condition here to $\alpha_A \neq \alpha_B$, but $\alpha_A \approx \alpha_B$.

Making the change of state variables of x_A and x_B to the new variables, corresponding to the sum and the difference of the number of foragers that visit the two options, that is, by defining,

$$x = x_A + x_B, \quad y = x_A - x_B, \tag{8}$$

we obtain an equivalent system of model equations. In fact, after successively adding and subtracting Eqs. (6) and (7), and by introducing the notation given in Eq. (8), the deterministic part of the foraging balance equations, guided by

pheromone trails towards two food sources, can be expressed as follows:

$$\frac{dx}{dt} = \left(\beta(n-x) - \frac{s}{s+x}\right)x, \tag{9}$$

$$\frac{dy}{dt} = \left(\beta(n-x) - \frac{s}{s+x}\right)y. \tag{10}$$

These equations have the general form of a recruitment-abandonment balance equation. The contributions of successful explorers are not considered at this time, since their random searches do not involve the pheromone trails, so we can express:

$$\frac{dx}{dt} = (R(x) - A(x))x, \tag{11}$$

$$\frac{dy}{dt} = (R(x) - A(x))y. \tag{12}$$

The steady-state solutions of Eq. (11) are obtained from the condition of permanent behavior of the state variable, $dx/dt = 0$, or,

$$(R(x) - A(x))x = 0. \tag{13}$$

From this last condition, it follows that two cases can occur $x = 0$, or according to Eq. (9):

$$\beta(n-x)(s+x) - s = 0. \tag{14}$$

The roots of the polynomial in Eq. (14) are easily obtained directly by some algebra calculations,

$$x_\pm = \frac{(n-s) \pm \sqrt{(n+s)^2 - 4\frac{s}{\beta}}}{2}. \tag{15}$$

This result is valid for $n \geq n_c$ where $n_c = 2\sqrt{s/\beta} - s$ is the critical density of the colony that comes from the positive radicand condition in Eq. (15). The system parameters β and s correspond to $R(x)$ and $A(x)$, the contributions of mass recruitment and mass abandonment. In addition, we must keep in mind the dependence $x_\pm = x_\pm(n)$ on the colony size. Later we consider $s = 10$ and $\beta = 0.00015$, then $n_c = 2\sqrt{s/\beta} - s \cong 500$ individuals. It is worth noting that $x_c = x_\pm(n_c) = \sqrt{s/\beta} - s$.

In the region before the bifurcation $n < n_c$, there are equal numbers of foragers visiting A and B. This means that the steady-state values are equal, *i.e.*, $x_+ = x_-$. In this case, Eq. (14) determines a line passing through the origin and point (n_c, x_c) with $x_c = (n_c - s)/2$. This last equation is the general form of the steady-state solutions for $n < n_c$.

Taking into account the above considerations, we include the steady-state solutions valid for the whole range of possible colony sizes,

$$x_\pm(n) = \begin{cases} \dfrac{n-s}{2} & n < n_c \\ \dfrac{(n-s) \pm \sqrt{(n+s)^2 - 4\frac{s}{\beta}}}{2} & n \geq n_c \end{cases}. \tag{16}$$

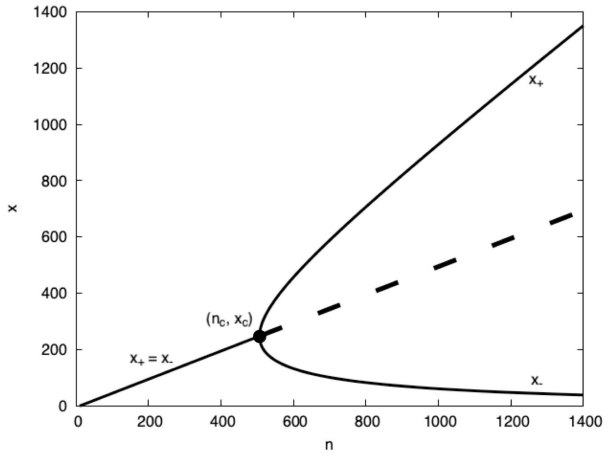

FIGURE 6. Bifurcation diagram of the steady-state solutions.

According to Eq. (16), the steady states depend on the colony size, which is represented in the bifurcation diagram in Fig. 6. The critical point behaves as a bifurcation point that separates the graph into two regions with homogeneous (equal number of individuals) and inhomogeneous (different number of individuals) visits to sources A and B.

Now, let us consider Eq. (10), which for convenience we express as follows,

$$\frac{dy}{dt} = \left(\frac{p(x)}{s+x}\right)y. \tag{17}$$

Here $p(x)$ is the polynomial of Eq. (14) which can be expressed in terms of its roots x_- and x_+. This means that Eq. (17) has an alternative form,

$$\frac{dy}{dt} = \left(\frac{(x-x_-)(x-x_+)}{s+x}\right)y. \tag{18}$$

The expressions for x_- and x_+ are given in Eq. (16). The variable y represents the difference in the number of individuals visiting two options A and B, and is therefore a measure of the symmetry features during the collective task.

Considering that the state variables x and y vary temporally at different scales (see Sec. 1), and that the system is close to the critical density n_c, the quasi-steady-state hypothesis can be adopted. In this case, the slow variation of the state variable associated with the total number of forage ants allows us to introduce the following approximation,

$$x \approx \phi. \tag{19}$$

We have introduced ϕ as a control parameter of the system model [9]. Under these conditions, Eq. (18) can be transformed into a one-variable differential equation for y, *i.e.*,

$$\frac{dy}{dt} = \left(\frac{(\phi-\phi_-)(\phi-\phi_+)}{s+\phi}\right)y, \tag{20}$$

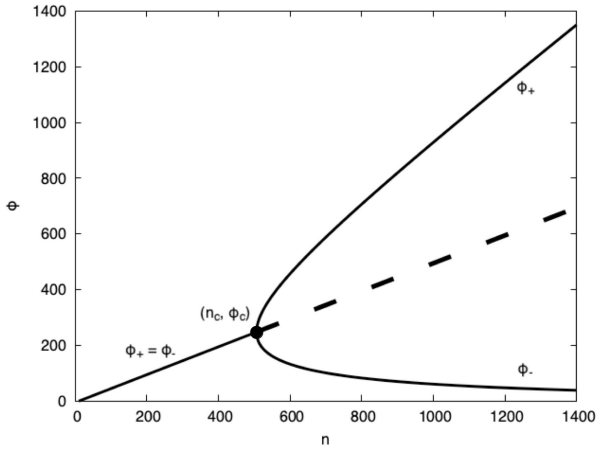

FIGURE 7. Bifurcation diagram of the model's control parameter.

where $\phi_\pm = \phi_\pm(n)$ are the roots of the polynomial in Eq. (17),

$$\phi_\pm(n) = \begin{cases} \dfrac{n-s}{2} & n < n_c \\ \dfrac{(n-s) \pm \sqrt{(n+s)^2 - 4\frac{s}{\beta}}}{2} & n \geq n_c \end{cases}. \quad (21)$$

The critical value of the control parameter can be evaluated directly by replacing the critical density in Eq. (21), that is, $\phi_c = \phi(n_c)$ (see Fig. 7).

By introducing the definition of the deterministic balance coefficient, we can write Eq. (20) in a simplified manner as a first-order linear differential equation with constant coefficient, *i.e.*,

$$\frac{dy}{dt} = K_1(\phi)y, \quad (22)$$

where,

$$K_1(\phi) = \left(\frac{(\phi - \phi_-)(\phi - \phi_+)}{s + \phi} \right). \quad (23)$$

According to Ref. [9] we can graphically examine the dynamic stability of y in Eq. (22) by introducing a potential function $U(y)$ such,

$$\frac{dy}{dt} = -\frac{\partial U(y)}{\partial y}. \quad (24)$$

In case of Eq. (22) the primitive function is given by Eq. (25),

$$U(y) = -\frac{1}{2}K_1(\phi)y^2. \quad (25)$$

Let us insist that $K_1 = R - A$ represents the balance of recruitment-abandonment near the critical region of steady-states. Figure 8 shows that in the stable region, the foraging population tends to visit A and B with the same number of individuals.

Convergent solutions of Eq. (22), with finite values of y in steady-state, are obtained by imposing the condition $K_1 \leq 0$, which means that ϕ is in the interval $[\phi_-, \phi_+]$ (see Fig. 7).

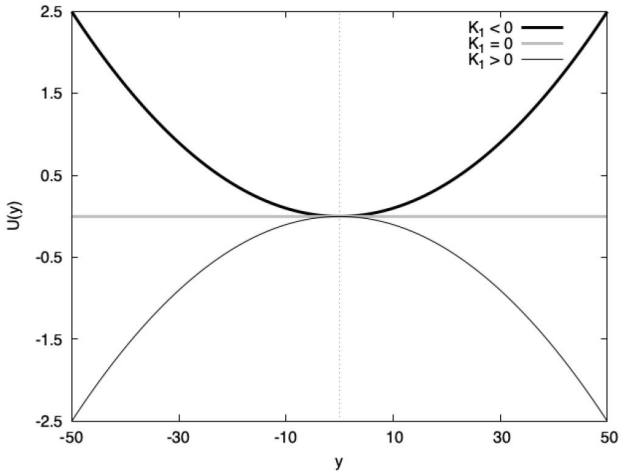

FIGURE 8. Potential stability function.

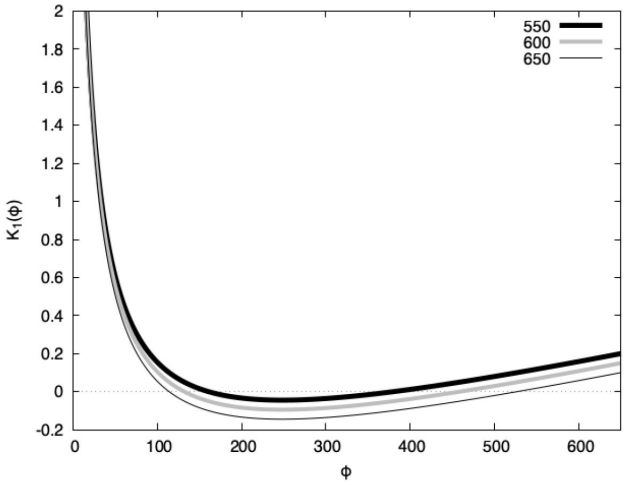

FIGURE 9. $K_1(\phi)$ coefficient for three different colony sizes.

TABLE I. Minimum values of $K_1(\phi)$ in the stable region.

n	ϕ_-	ϕ_+	$\phi_{\min}$	$K_1(\phi_{\min})$
550	161.7	378.3	248	-0.04
600	132.6	457.3	248	-0.09
650	114.7	525.5	248	-0.14

Although there is no general rule, an appropriate choice of the controlling parameter ϕ can be facilitated by using as a guide the $K_1(\phi)$ plots obtained from Eq. (23). Some examples considering densities close to critical density are represented in Fig. 9. Table I includes the x-axis cut-off points ϕ_- and ϕ_+, in addition to the minimum values of the ϕ parameter. A reasonable choice could be the parameter $\phi(n) = \phi_{min}$ at different colony density sizes.

In the following, we consider an extension of the parameter analysis according to Ref. [9]. In this reference, the author considers $\phi = 2.7$ as a reasonable choice of the control parameter, since this value is close to the critical point $\phi_c = 2$.

This means,

$$\phi \gtrsim \phi_c. \tag{26}$$

The selection has two conditions: a) ϕ is greater than ϕ_c, and b) ϕ is close to ϕ_c. Here we present a particular case for selecting the parameter $\phi = \phi(n)$ and therefore of the coefficient evaluation K_1 in Eq. (23). In this way, we have a consistent model using Eqs. (22) and (23). Only the colony size, recruitment, and abandonment parameters are needed for the symmetry model to be well defined.

We first evaluate the critical value of the control parameter of the model,

$$\phi_c = \phi(n_c). \tag{27}$$

For this, we substitute the critical density in Eq. (21), that is,

$$\phi_c = \phi(n_c) = \begin{cases} \dfrac{n_c - s}{2} \\ \dfrac{(n_c - s) \pm \sqrt{(n_c + s)^2 - 4\frac{s}{\beta}}}{2}. \end{cases} \tag{28}$$

Using the relation $n_c = 2\sqrt{s/\beta} - s$ of the critical density in Eq. (28), the critical control parameter can be expressed in terms of the recruitment-abandonment parameters,

$$\phi_c = \sqrt{\frac{s}{\beta}} - s. \tag{29}$$

Figure 10 shows the point (n_c, ϕ_c) and the point marked as (n, ϕ) that we have chosen to construct a specific example following the steps in the previous discussion. We start with the proposal in Eq. (30),

$$n = n_c + 2s. \tag{30}$$

Substituting the critical density n_c in Eq. (30), we obtain

$$n = 2\sqrt{\frac{s}{\beta}} + s. \tag{31}$$

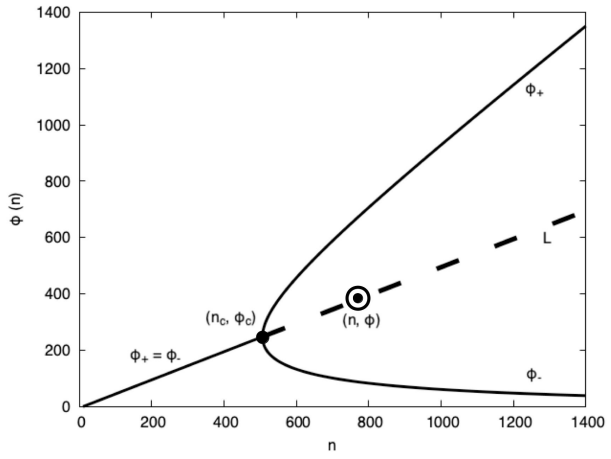

FIGURE 10. Selection of the model's control parameter.

On the other hand, located on the line L in Fig. 10, it is true that

$$\phi = \frac{n - s}{2} = \sqrt{\frac{s}{\beta}}. \tag{32}$$

We check the conditions imposed on the control parameter for its critical value, that is, it satisfies,

$$\phi = \sqrt{\frac{s}{\beta}} \gtrsim \phi_c = \sqrt{\frac{s}{\beta}} - s. \tag{33}$$

Subsequently, we evaluate $\phi_\pm(n)$ at the density given above, in Eq. (30), $n = n_c + 2s$ which according to Eq. (21) results in

$$\phi_\pm(n) = \sqrt{\frac{s}{\beta}} \pm \sqrt{2s\sqrt{\frac{s}{\beta}} + s^2}, \tag{34}$$

from which we obtain directly, from Eqs. (32) and (34), the relation,

$$\phi - \phi_\pm = \pm\sqrt{2s\sqrt{\frac{s}{\beta}} + s^2}. \tag{35}$$

With these results in hand, we can evaluate the coefficient K_1 of Eq. (23) in terms of the recruitment-abandon parameters, *i.e.*,

$$K_1 = -\frac{\sqrt{2s\sqrt{\frac{s}{\beta}} + s^2}\sqrt{2s\sqrt{\frac{s}{\beta}} + s^2}}{s + \sqrt{\frac{s}{\beta}}}. \tag{36}$$

Simplifying this expression and combining the result with Eq. (22), we conclude that

$$\frac{dy}{dt} = K_1 y, \tag{37}$$

being

$$K_1 = -\frac{\left(2\sqrt{\frac{s}{\beta}} + s\right) s}{\sqrt{\frac{s}{\beta}} + s}. \tag{38}$$

If we recall that $s = 10$ and $\beta = 0.00015$ represent the system's parameters, the coefficient K_1 in Eq. (38) can be directly substituted in Eq. (37) to complete the description of the deterministic component of the model. By presenting this specific example, we show a step-by-step methodology for determining the "deterministic" component of the foraging task. Eq. (22) and (23) constitute a frame upon which the effect of internal or external random noise can act to produce a preferential choice between the two options A and B. This occurs when the ant colony establishes a steady-state equilibrium of recruitment-abandonment balance when forming pheromone trails during foraging.

4. Symmetry breaking

According to Eq. (22), and after imposing the condition $K_1 \leq 0$, the symmetry function defined as the difference in the number of foragers between sources A and B, *i.e.*, the

state variable $y = y(t)$, tends exponentially to zero at long times by considering only the deterministic component of the model. In this case, options A and B present the same number of individuals. To break this symmetry, we propose to add to the balance equation Eq. (22) an intrinsic noise term of the system associated with the population of successful explorers, *i.e.*

$$\frac{dy}{dt} = K_1 y + K_2 \delta F(t), \tag{39}$$

where

$$K_2 = \alpha(n - \phi). \tag{40}$$

The factor K_2 results after the subtraction of Eqs. (6) and (7) including the approximation in Eq. (19). Hence, Eq. (39) complemented by Eq. (40) has the general form of the balance equation Eq. (5). The random feature of independent searches is represented by the factor $\delta F(t)$, with time-dependent white noise values associated with the randomness of the foraging due to successful explorers.

At this point, we assume that Eq. (39) corresponds to a Langevin equation for the foraging symmetry with Gaussian white noise and uncorrelated perturbations, *i.e.*,

$$\langle \delta F(t) \rangle = 0, \tag{41}$$

$$\langle \delta F(t) \delta F(t') \rangle = \delta(t - t'), \tag{42}$$

where $\langle\, \rangle$ represents the average over short time intervals [12]. We consider the above equations as a starting point for a first analysis of the symmetry breaking in the number of foragers during the choice of sources A or B. In fact, the solution to the Langevin equation Eq. (39) is

$$y(t) = y(0) e^{K_1 t} + K_2 \int_0^t \delta F(t') e^{K_1 (t - t')} dt', \tag{43}$$

from here it follows,

$$\langle y(t) \rangle = y(0) e^{K_1 t}. \tag{44}$$

The first term in the expression for $y(t)$ represents the free response of the colony to allocate the same number of forages in identical sources A and B. The second term confirms that the exploration process has the characteristics of a random disturbance (intrinsic random noise), which is the origin of foraging symmetry-breaking.

Furthermore, the symmetry correlation function evaluated thorough Eq. (43), is given by Eq. (45),

$$\langle y(t) y(t') \rangle = \frac{K_2}{K_1} e^{K_1 |t - t'|}. \tag{45}$$

The symmetry is exponentially autocorrelated in time with $\tau_{\text{relax}} = K_1^{-1}$, the characteristic relaxation time. The mean square symmetry turns out to be

$$\left\langle y^2(t) \right\rangle = y^2(0) e^{2K_1 t} + \frac{K_2}{K_1}(1 - e^{2K_1 t}). \tag{46}$$

For long times $t \gg K_1^{-1}$, the steady-state condition of this parameter is obtained,

$$\left\langle y^2(t) \right\rangle = \frac{K_2}{K_1}. \tag{47}$$

The fluctuations associated with the symmetry $y(t)$ are calculated by using the usual definition,

$$\left\langle (\delta y(t))^2 \right\rangle = \left\langle y^2(t) \right\rangle - \langle y(t) \rangle^2. \tag{48}$$

Substituting Eqs. (44) and (47) in Eq. (48), we have

$$\left\langle (\delta y(t))^2 \right\rangle = \frac{K_2}{K_1}(1 - e^{2K_1 t}). \tag{49}$$

Finally, we see that the fractional fluctuations satisfy the relation,

$$F_r = \left(\frac{\left\langle (\delta y(t))^2 \right\rangle}{\left\langle y^2(t) \right\rangle} \right)^{\frac{1}{2}} = 1. \tag{50}$$

In this case, $F_r = 1$ means that the fluctuations generated by the intrinsic noise concern the current value of the symmetry that leads to uncertainty. The mean square symmetry value has statistical significance only when $F_r \ll 1$; however, when $F_r = 1$, the fluctuations are not smoothed out (they maintain their appearance of random spikes) even when the average $\left\langle y^2(t) \right\rangle$ increases [13].

It is noteworthy that in the majority of the previous results, the quotient in Eq. (51) appears frequently,

$$\Phi(\phi) = \frac{K_2}{K_1}. \tag{51}$$

This quotient contains the foraging parameters, including the rate of successful explorers and the colony size. It also explicitly depends on the control parameter of the model ϕ as a rational homographic function, *i.e.*,

$$\Phi(\phi) = \frac{\alpha(n - \phi)(s + \phi)}{(\phi - \phi_-)(\phi - \phi_+)}. \tag{52}$$

We find that this parameter can be considered an order parameter that relates the dual effect processes of no-trail foraging (successful exploration) to trail foraging (recruitment-abandonment) in an order-disorder balance. In this sense, $\Phi(\phi)$ represents the mechanism of the underlying effects of the collective task, since it measures the balance between the deterministic and random components of the collective foraging task (see Fig. 11).

Figure 11 shows the parameter $\Phi(\phi)$ as a function of the control parameter of the model ϕ at a fixed colony size. The maximum of the rational homographic function, on the negative branch of the graph, moves upwards from critical density; at the same time, the points ϕ_- and ϕ_+ move further apart as the colony size increases.

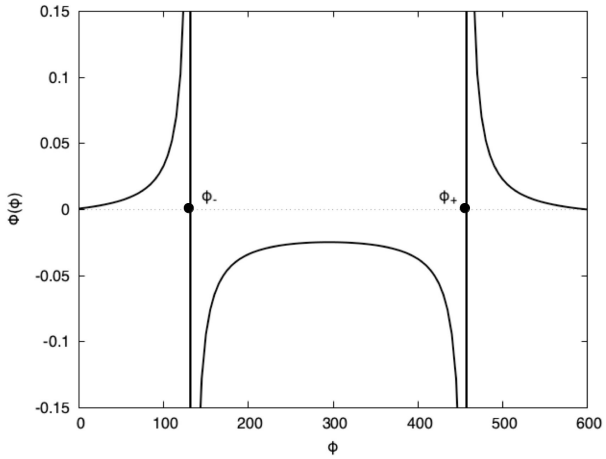

FIGURE 11. Order parameter of the order-disorder balance for a fixed colony size of 600 individuals.

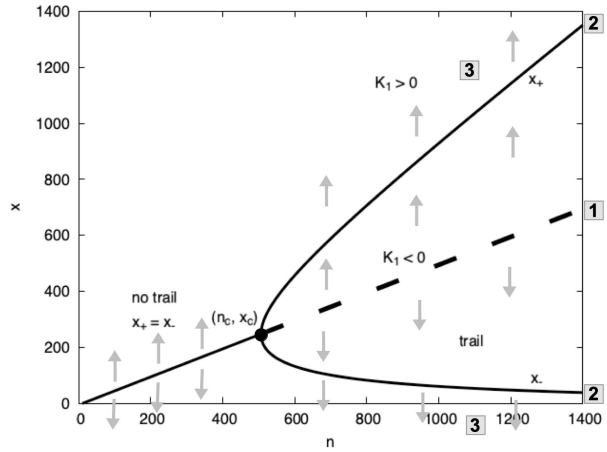

FIGURE 12. Intrinsic noise effects.

5. Euler-Maruyama analysis

Based on the deterministic component of the model, we can consider the noise effects during the foraging activity of an ant colony. At this point, we clarify how noise allows the system to transition between steady-states. Figure 12 represents the successful explorers present at any density in **1**. In the presence of intrinsic noise in the system, this population is attracted to recruit to one of the tracking paths **2** defined by x_- or x_+ in a region where $n \geqslant n_c$. The region **3** corresponds to the simple explorers who abandon the task; these individuals must be distinguished from the successful explorers on line **1**.

To describe noise-induced spontaneous symmetry breaking in more detail, we will numerically solve Eq. (39). The discretized form of the Langevin equation is obtained by converting this equation into its corresponding discrete difference form. The result is the expression known as the Euler-Maruyama algorithm [14],

$$y_{m+1} = (1 - K_1\tau)y_m + \sqrt{K_2\tau}F_m, \qquad (53)$$

FIGURE 13. Symmetry-breaking behavior by preferential visits to an option.

TABLE II. Simulation model parameters taken from literature.

Parameter	Value	Description
α	0.0052	Exploration rate (min^{-1})
β	0.00015	Recruitment rate (min^{-1})
s	10	Max abandonment rate (min^{-1})
n	[100, 1200]	Ant's colony size interval

here F_m is a random variable generated from a normal distribution, $N(0,1)$ with mean zero and standard deviation equal to one, which is taken randomly at each step τ of the simulation with $m = 1, 2, 3, ...$

In the following, we apply the algorithm in Eq. (53) to analyze symmetry breaking in the context of consensus collective decision-making in a pheromone-guided foraging ant colony [1,2,4]. Table II shows the parameters used in the simulation. The values for K_1 and K_2 are evaluated in agreement with their definitions, Eqs. (21), (23), and (40) in the previous section. Each of the simulations obtained is presented below, which requires an appropriate choice for the control parameter of the model and the colony size.

As a first algorithm application, Eq. (53), we consider the behavior of preference visits between two identical options A and B as shown in Fig. 13. Figure 14 presents the results of reproducing the expected behavior of episodic visits considering two foraging options. To simulate this behavior, we have considered specific values for the model parameters, we use $K_1 = 0.1$, $K_2 = 6$, $n = 600$, and $\tau = 0.1$. The perturbations generated during the collective task produce alternating visits between food sources A and B within the deterministic steady-state frame (see Fig. 12).

Subsequently, after performing repeated experiments, we generated a series of histograms that captured the effects of increasing noise intensity K_2 in Eq. (53), considering two situations: at densities below and above the critical density.

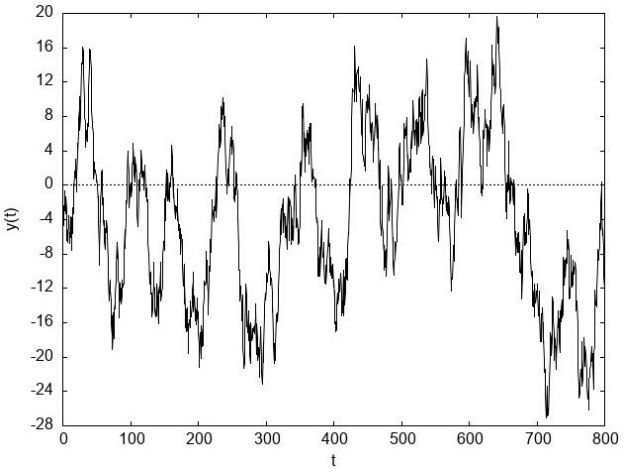

FIGURE 14. Episodic random visiting behavior at two identical options A and B.

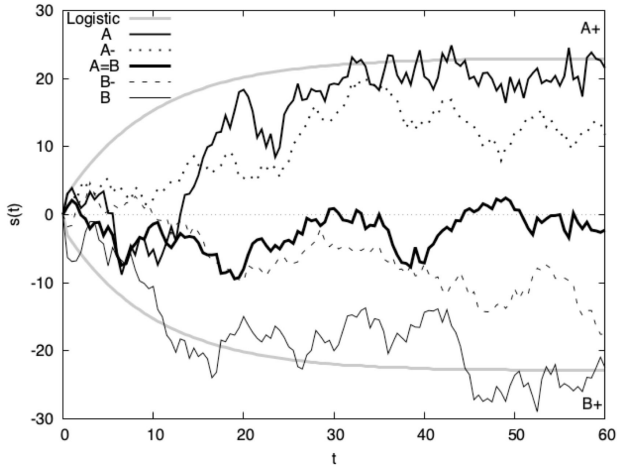

FIGURE 15. Possible random curves generated by successive runs of the simulation algorithm.

Figure 15 shows the possible results of applying the Euler-Maruyama algorithm. By convention, if the colony simultaneously visits both exploitation options, we denote it as $A = B$. If it prefers one option, only A or B is indicated. These runs coincide with the logistic curve from analytically solving Eq. (39) after making $\delta F(t) = 1$. The indecision random curves have intermediate values that fall outside the range of the logistic curves; these runs are denoted as $A-$, $A+$, $B-$, $B+$.

In the first case, $n < n_c$, with 400 individuals, pheromone trails have not yet formed, and the foraging by successful explorers dominates the collective behavior. The effect of noise breaking the symmetry induces moving from $A = B$ to $A > B$ or $A < B$. Figure 16 shows the histograms resulting from experiments with different noise intensities. As the value of K_2 increases, the central bar $A = B$ decreases, while the side bars increase separately. The symmetry is broken, since the tendency $A > B$ or $A < B$ increases as the two options are visited alternately. In this case, indecision bars are not observed. The values used in the simulation are $n = 400$, $K_1 = 0.3$, and $K_2 = 1, 2, 3, 6$.

In a second case, $n > n_c$, setting 600 individuals, pheromone trails have already been established, and the foraging by recruitment-abandonment dominates the collective behavior. Figure 17 shows histograms for many runs of the algorithm, in Eq. (53), as the noise intensity increases. The central bar $A = B$ starts at a lower height than the side bars A or B. The symmetry is broken from the beginning of the simulation, with alternating visits between options A and B. As the noise intensity increases, the central bar decreases even further while the side bars tend towards $A \geqslant B$. In this case, changes in the height of A or B are better perceived, showing a preference for one option; some indecision bars are also presented. The values used in the simulation are $n = 600$, $K_1 = 0.1$, and $K_2 = 1, 2, 3, 6$.

In some applications of collective behavior, it has been suggested that sloping at the midpoint of the cumulative distribution function, represented as a line superposed to the histograms in Figs. 16 and 17, measure the stability of the colony's collective decision-making towards either option A or B [15, 16]. In Fig. 16, where the condition $n < n_c$ is satisfied, the slope of the midpoint of the cumulative distribution decreases with increasing noise intensity, showing that the choice from the options is weakly stable. However, in Fig. 17, under the condition $n > n_c$, the slope of the midpoint of the cumulative distribution increases with increasing noise intensity, indicating a tendency towards a stable consensus choice by the colony on one of the options A or B.

In summary, we have shown that even when the colony faces two identical options, A and B, intrinsic noise generated by successful foragers breaks the symmetry in the choice of options during the collective task. A series of simulation runs indicates evidence of consensus on collective decision-

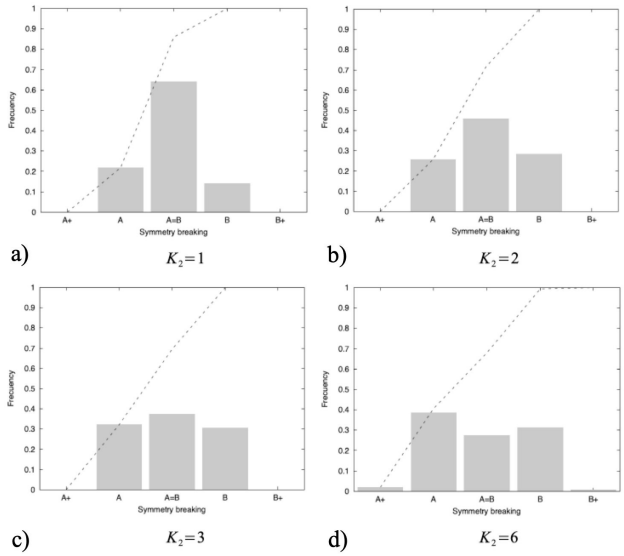

FIGURE 16. Noise affects the symmetry-breaking behavior of the forager's number in each option A and B without pheromone trails.

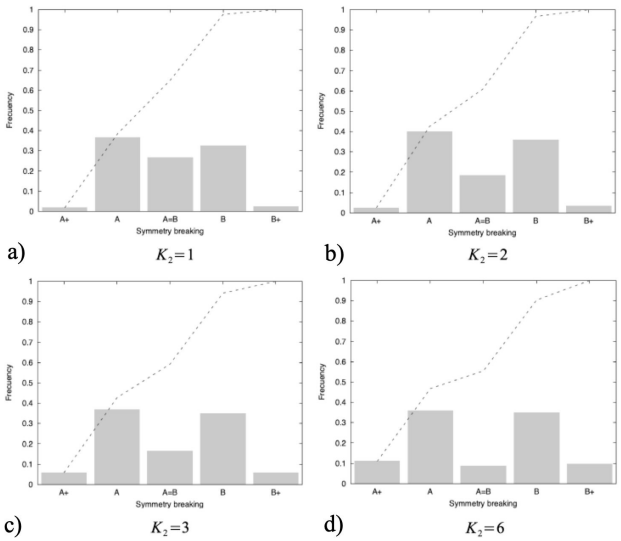

FIGURE 17. Noise affects the symmetry-breaking behavior of the forager's number in each option A and B with pheromone trails.

making to visit options A or B, at densities above the critical density.

6. Conclusions

Many ant colonies exhibit several self-organization behaviors when performing the collective foraging task. Foraging in multiple food sources leads to various flexible behaviors that adapt to environmental conditions. In this paper, we consider a system of nonlinear differential equations to describe the collective foraging task of an ant colony visiting two identical food sources in a static environment. The model consists of a deterministic part, a recruitment-abandonment balance during the formation and maintenance of pheromone trails, and a random part, that considers intrinsic noise associated with successful foragers that perform foraging tasks independently of the pheromone trails.

Analysis of the deterministic part of the model, in the absence of perturbations, leads to a bifurcation diagram of the steady-state solutions. The competition to visit one of the two options arises at the bifurcation point at the critical density. The deterministic component is a framework for the random component to generate transitions between the different steady-states. Successful exploration generates perturbations that act as intrinsic noise derived from variations within the system. A fundamental property of self-organized collective decision-making is the symmetry breaking during task development. The state variable for symmetry breaking satisfies a Langevin equation. Analysis of this equation leads to an order parameter that represents the mechanism of the effects underlying the collective task by balancing the participation of the deterministic and random components of the system.

We solved the Langevin equation numerically and verified that the colony makes random episodic visits to both options. In the region of densities lower than the critical density, the colony allocates the same number of forages to each option. As noise intensity increases, the symmetry is broken, generating alternating random visits of low stability between the two options. In the region of densities above the critical density, the colony breaks the symmetry with alternating visits between the two options. This tendency is increased by increasing noise intensity, since the stability of the decision improves. We found that the symmetry-breaking process, which statistically tends toward the preferential choice of one of the options, instead of exploiting both sources simultaneously, can be generated by the effects of the intrinsic noise of the colony.

1. M. Beekman, D.J. Sumpter, and F.L. Ratnieks, Phase transition between disordered and ordered foraging in Pharaoh's ants, *Proc. Natl. Acad. Sci.* **98** (2001) 9703, https://doi.org/10.1073/pnas.161285298
2. D.J. Sumpter, and M. Beekman, From nonlinearity to optimality: pheromone trail foraging by ants, *Anim. Behav.* **66** (2003) 273, https://doi.org/10.1006/anbe.2003.2224
3. C. Grueter, R. Schuerch, T.J. Czaczkes, K. Taylor, T. Durance, S.M. Jones, and F. L. Ratnieks, Negative feedback enables fast and flexible collective decision-making in ants, *PloS One* **7** (2012) e44501, https://doi.org/10.1371/journal.pone.0044501
4. A. Dussutour, M. Beekman, S.C. Nicolis, and B. Meyer, Noise improves collective decision-making by ants in dynamic environments, *Proc. R. Soc. B: Biol. Sci.* **276** (2009) 4353, https://doi.org/10.1098/rspb.2009.1235
5. C. Grüter, T.J. Czaczkes, and F.L. Ratnieks, Decision-making in ant foragers (Lasius niger) facing conflicting private and social information, *Behav. Ecol. Sociobiol.* **65** (2011) 141, https://doi.org/10.1007/s00265-010-1020-2
6. M. Lehue, and C. Detrain, Foraging through multiple nest holes: An impediment to collective decision-making in ants, *PloS One* **15** (2020) e0234526, https://doi.org/10.1371/journal.pone.0234526
7. E.J. Robinson, O. Feinerman, and N.R. Franks, Experience, corpulence and decision-making in ant foraging, *J. Exp. Biol.* **215** (2012) 2653, https://doi.org/10.1242/jeb.071076
8. J.S. Miller, and N. Pinter-Wollman, Social interactions differ in their impact on foraging decisions, *Anim. Behav.* **203** (2023) 183, https://doi.org/10.1016/j.anbehav.2023.07.008
9. S.C. Nicolis, Fluctuation-induced symmetry breaking in a bistable system: a generic mechanism of selection between competing options, *Int. J. Bifurcation Chaos* **14** (2004) 2399, https://doi.org/10.1142/S0218127404010667

10. S.C. Nicolis, and A. Dussutour, Self-organization, collective decision-making and resource exploitation strategies in social insects, *Eur. Phys. J. B* **65** (2008) 379, https://doi.org/10.1140/epjb/e2008-00334-3

11. J. Pasteels, J.L. Deneubourg, and S. Goss, From individual to collective behavior in social insects, vol. 54 (Experientia Supplementum, BirkhaÃ¼ser, Basel, 1987), pp. 155-175, http://hdl.handle.net/2013/ULB-DIPOT:oai:dipot.ulb.ac.be:2013/125221

12. R. Zwanzig, Nonequilibrium statistical mechanics, (Oxford University Press, New York, USA, 2001), pp. 3-29, https://doi.org/10.1093/oso/9780195140187.002.0001

13. C. Kittel, and R.W. Hill, Thermal physics, 1st Ed. (John WIley & Sons Inc., New York, USA, 1970), pp. 175-179.

14. T. Tomé, and M.J. De Oliveira, Stochastic Dynamics and Irreversibility, 1st Ed. (Springer International Publishing, Switzerland, 2015), pp. 43-57.

15. H. Hamann, B. Meyer, T. Schmickl, K. Crailsheim, A Model of Symmetry Breaking in Collective Decision-Making, 11th Int. Conf. Simul. Adapt. Behav., vol. 6226 (Springer Nature Link, Berlin, Heidelberg, 2010), pp. 639-648, https://doi.org/10.1007/978-3-642-15193-4_60

16. H. Hamann, T. Schmickl, H. Wörn, and K. Crailsheim, Analysis of emergent symmetry breaking in collective decision-making, *Neural Comput. & Appl*. **21** (2012) 207, https://doi.org/10.1007/s00521-010-0368-6